Russian Journal of Earth Sciences Online ISSN: 1681-1208

Special Issue: "Kamchatka Earthquake M 8.8 on July 29, 2025"

Stress-Strain State of the Lithosphere of the Kamchatka Pacific Coast Before the July 29, 2025 Earthquake

A. Yu. Polets[1,*], Yu. L. Rebetsky[2], and V. A. Gavrilov[3,4]

[1] Institute of Marine Geology and Geophysics Far Eastern Branch Russian Academy of Sciences (IMGG FEB RAS), Yuzhno-Sakhalinsk, Russian Federation
[2] Schmidt Institute of Physics of the Earth of the Russian Academy of Sciences (IPE RAS), Moscow, Russian Federation
[3] Institute of Volcanology and Seismology of the Far Eastern Branch of the Russian Academy of Sciences (IVS FEB RAS), Petropavlovsk-Kamchatsky, Russian Federation
[4] Vitus Bering Kamchatka State University, Petropavlovsk-Kamchatsky, Russian Federation
* **Correspondence to:** A. Yu. Polets, a.polec@mail.ru

Abstract: On July 29, 2025, an earthquake with a moment magnitude of M_W 8.8 occurred off the coast of Kamchatka, becoming the strongest in the Kamchatka seismofocal zone since 1952. With the aim of reconstructing the parameters of the modern stress field of the Earth's crust on the Pacific coast of Kamchatka prior to this event, a new modification of the cataclastic analysis method of discontinuous displacements was applied. Stress determination was performed based on earthquake focal mechanism data. The calculations of the stress tensor components were carried out within domains identified as quasi-homogeneous in their deformation state. Each such domain corresponded to its own homogeneous dataset of earthquakes. The results of the stress reconstruction obtained in the study region revealed characteristic features of the spatiotemporal distribution of the stress state parameters. Based on the analysis of the stress state, seismotectonic domains with different deformation regimes were identified. A significant feature of the stress field is associated with the junction area of the Aleutian and Kamchatka seismofocal zones, where the main heterogeneities of the stress field are observed.

Keywords: Tectonic stress, focal mechanism, method of cataclastic analysis, Kamchatka megathrust earthquake

Citation: Polets A. Yu., Rebetsky Yu. L., and Gavrilov V. A. (2026), Stress-Strain State of the Lithosphere of the Kamchatka Pacific Coast Before the July 29, 2025 Earthquake, *Russian Journal of Earth Sciences*, 26, ES2013, EDN: YNHECB, https://doi.org/10.2205/2026es001123

Research Article

Received: February 2, 2026
Accepted: May 25, 2026
Published: July 1, 2026

1. Introduction

The Kuril-Kamchatka island arc extends for 2,000 km – from the Kamchatka Isthmus to Hokkaido Island. Of this total, 800 km comprise the Kamchatka Peninsula and 1,200 km for the Kuril Islands. The Kamchatka segment of the island arc is one of the most seismically active regions on Earth and has a complex structure of the seismic focal zone.

The high seismicity is associated with the surface outcrops of the focal zone (a fault system). The focal zone intersects all the coastal structures of eastern Kamchatka and runs almost parallel to the deep-sea trench and the volcanic belt. At the surface, its width reaches 200 km, from the deep-sea trench to the Kamchatka coast. At a depth of 70 km, the width of the seismic focal zone decreases to 20 km. Beneath the eastern shore of Kamchatka, it is truncated by steeply dipping faults that extend to depths of up to 110 km. Shallow earthquakes occur near these faults. Beneath the coast, the depth of their hypocenters reaches 60 km.

The focal depth increases to 100 km beneath the East Kamchatka Range, and to 200–300 km beneath the Sredinny Range. Rare earthquakes have depths of 300–500 km beneath Western Kamchatka [*Aprodov*, 2000].

A characteristic feature of the tectonic structure of eastern Kamchatka is the presence of large structures oriented at an angle to the direction and strike of the island arc. These are uplifts – the peninsulas (Shipunsky, Kronotsky, and Kamchatsky Cape) and depressions – the bays (Avacha, Kronotsky, and Kamchatsky). In the areas of the eastern Kamchatka peninsulas, the number of earthquakes in the focal zone increases by 1.5–2 times compared to the average level for the seismic focal zone. It is here that the intensity of modern fault movements reaches the maximum level on Earth. Accordingly, the strongest earthquakes occur in the ocean near the Kamchatsky, Kronotsky, and Shipunsky peninsulas.

From January 2015 to June 2025, six strong earthquakes with $M_W \geq 7.0$ occurred off the coast of Kamchatka, as well as one earthquake near the Commander Islands (Figure 1).

On July 30 at 11:24 local time (July 29 at 23:24 UTC), the strongest earthquake in the history of observations occurred 150 km east of Petropavlovsk-Kamchatsky, with a moment magnitude (M_W) of 8.8 (according to the Global Centroid Moment Tensor (GCMT) catalog). Prior to this, the 1952 Kamchatka earthquake was considered the strongest in the studied region; its hypocenter was located 130 km from Cape Shipunsky and had a magnitude of M 9.0.

To date, the July 29 (30), 2025 earthquake with a magnitude of 8.8 is the strongest seismic event worldwide since the 2011 Tohoku earthquake (M_W 9.1). The July 29 (30), 2025 earthquake was preceded by 50 earthquakes with magnitudes exceeding 5.0, including an M_W 7.4 earthquake on July 20, 2025 (Figure 1), and three earthquakes with magnitudes of 6.6.

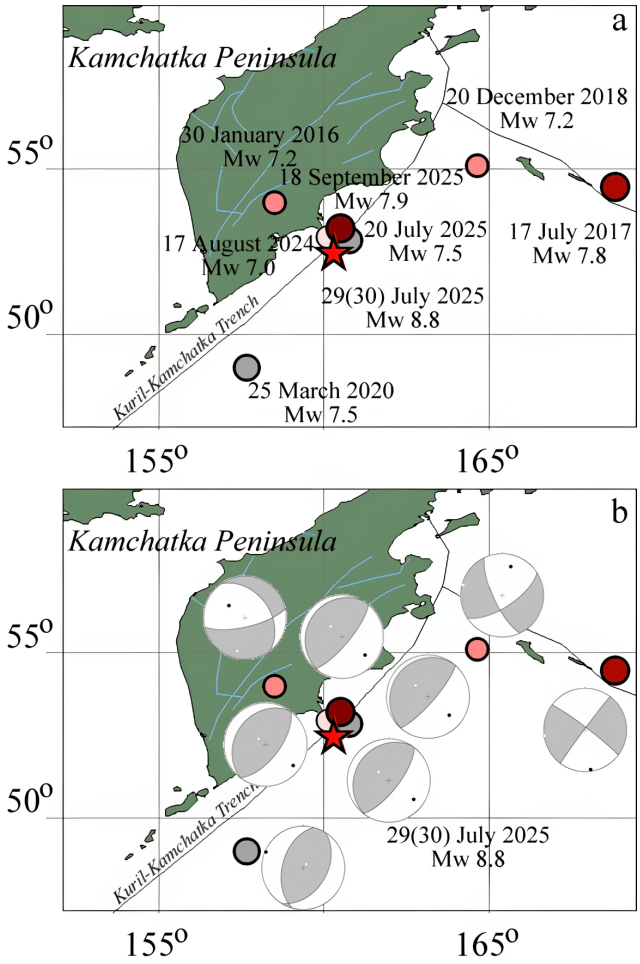

Figure 1. Map of epicenters for strong earthquakes ($M_W \geq 7.7$) for the period 2015–2025.

The occurrence of the strongest ($M_W \geq 7.7$) earthquake in the Avacha Bay area had been previously forecast in studies by [*Fedotov and Solomatin*, 2017, 2019; *Gavrilov et al.*, 2023].

In 2015, according to [*Chebrov et al.*, 2021], the overall seismicity in the region was at the background levels. The number of recorded events with $M_L \geq 3.5$ ($K_S \geq 8.5$) and strong earthquakes with $M_L \geq 5.0$ ($K_S \geq 11.5$) was close to the annual average. No anomalous or outstanding events were noted. An increase in seismicity for the Kamchatka and Commander Islands catalog was reported in the study by [*Chebrov et al.*, 2023]; the number of recorded events in 2018–2019 with $M_L \geq 3.5$ ($K_S \geq 8.5$) and strong earthquakes with $M_L \geq 5.0$ ($K_S \geq 11.5$) exceeded was 1.5 times the annual average. Two seismic zones contributed most significantly to the deviation from the annual averages: the Pacific Ocean and the Shelikhov Bay. The December 20, 2018 magnitude 7.2 (Figure 1) earthquake resulted in the released seismic energy for the Pacific Ocean zone exceeding the annual average by more than two orders of magnitude.

The July 29 (30), 2025 earthquake (M_W 8.8) was preceded by a strong earthquake on August 17 (18), 2024. The epicenter of this event was located off the eastern coast of the peninsula, 113 km from Petropavlovsk-Kamchatsky. The earthquake magnitude was 7.0.

The preparation of a strong earthquake is determined by the tectonic stress field. The Kamchatka earthquake of July 29 (30), 2025, provided a unique opportunity to study the characteristic features of the tectonic stress field that governed the development of large-scale rupture.

The aim of this study is to investigate the features of the stress state of the Pacific coast of Kamchatka preceding the Kamchatka earthquake of July 29 (30), 2025.

2. Methodology

The method of cataclastic analysis of discontinuous displacements (MCA) [*Rebetsky*, 2007] was applied to reconstruct the parameters of the modern stress field along the Pacific coast of Kamchatka. The method comprises several stages and, as a result of analyzing ensembles of earthquake focal mechanisms, allows for determining not only the orientation of the principal stress axes and the value of the Lode–Nadai coefficient but also the relative values of the maximum shear stresses and the effective confining pressure.

The algorithm of the method, which implements the principle of maximum dissipation of elastic strain energy, is similar to those used in the methods of [*Angelier*, 1984; *Gephart*, 1990; *Gephart and Forsyth*, 1984; *Michael*, 1984]. Its distinguishing feature is that it is applied only to those earthquake focal mechanisms that have passed a homogeneity test.

Stress determination was performed based on seismological data of earthquake focal mechanisms using the MCA in its new modification. The calculations utilized the software package STRESSseism_v.3.0 [*Rebetsky et al.*, 2024; *Rebetsky and Sycheva*, 2024]. The new MCA algorithm simultaneously implements two approaches: a graphical one–summation of areas where the greatest and least principal compressive stresses can be located [*Angelier and Mechler*, 1977; *Gushchenko*, 1996], and a numerical calculation involving finding the maximum of an optimization function [**3**; *Angelier*, 2002; *Etchecopar*, 1984; *Etchecopar et al.*, 1981; *Michael*, 1984].

The first approach differs from the right dihedron method [*Angelier and Mechler*, 1977] in that it relies not only on the fundamental premise of that approach, which requires a reduction in elastic energy as a result of each slip in the earthquake source, but also uses Ziegler's maximum principle in the theory of plasticity [*Nikitin and Yunga*, 1977]. A consequence of this principle is the requirement that, in the direction of the sought axes of greatest compression, each displacement along a fault should generate additional irreversible shortening strains, and in the direction of the least compressive (or tensile) stresses–elongation strains. In the direction of the intermediate principal stress, additional irreversible strains can be either shortenings or elongations, but their amplitudes must be smaller than those in the direction of the other two extreme principal stresses. Note

that the inequalities following from Ziegler's principle include the inequalities of the right dihedron method [*Angelier and Mechler*, 1977].

The latest modification of the MCA also utilizes the Wallace–Bott hypothesis [*Bott*, 1959; *Wallace*, 1951], but it is supplemented by the postulate that the slip planes relative to the principal stress axes should be oriented so as to minimize the work of friction forces on the displacements across the ensemble of faults. The study [*Rebetsky and Sycheva*, 2024] demonstrated that the optimization function constructed on the Wallace–Bott hypothesis is an analogue of the Mises function in the theory of true crystal plasticity, where friction forces are not accounted for; that is, it should be well-suited for describing metal failure, but not rock failure. For rocks, the strength limit is associated not only with overcoming cohesive strength but also with friction forces on faults. Therefore, the postulate adopted in the new modification of the cataclastic method regarding accounting for the orientation of fault planes relative to the principal stress axes and the ratio of the spherical and deviatoric components of the stress tensor implements a strength criterion for elastic-brittle media.

After the first stage, data on the principal stress axes and the value of the Lode–Nadai coefficient are determined. After the second stage, the maximum shear stress and effective pressure, normalized to an unknown but regionally constant effective cohesive strength, are determined. The calculations of the stress tensor components are performed within domains identified as quasi-homogeneous in their deformation state. Each such domain corresponds to its own homogeneous dataset of earthquake focal mechanisms. The modification of the optimization function implemented in the new version of the STRESSseism_v.3.0 program has reduced the required minimum number of events in a homogeneous dataset of focal mechanisms to 4–5 and limited their maximum number to 10 events.

3. Data and Stress Reconstruction Results

Focal mechanism solutions from the GCMT catalog were used as input data. The reconstruction was performed for the time interval from 1976 to 2025. A total of 363 mechanisms (depth range 0–30 km) were selected for calculating the parameters of the contemporary stress field. During the considered time period, the study region is characterized by both zones of high event density and zones with a low number of events. In cases where the epicenter density is sufficiently high, the MCA algorithm forms an initial dataset for a minimum gathering radius, with its subsequent sequential increase; this allows for stress reconstruction with the smallest averaging window size. In addition to events located within the gathering radius area, events remote from the calculation node can also be included in the initial dataset. This enables the formation of initial datasets for seismically active areas with low and heterogeneous earthquake density, utilizing both weak, closely spaced earthquakes and remote strong events.

For an earthquake with M = 6.0, the radius of elastic unloading should be about 30–40 km [*Dobrovolsky*, 1991]. A magnitude range of 4.7–6.5 was used in the calculations. Earthquakes with magnitudes of 6.5 and higher (17 events in total) were not used in the reconstruction.

The number of events in a homogeneous dataset ranged from 4 to 10. Processing of the initial seismological data was performed in a long-period reconstruction mode at grid nodes of 0.5°× 0.5° in the lateral direction for the depth interval of 0–30 km. Procedures for forming homogeneous datasets of earthquake focal mechanisms were completed for 86 quasi-homogeneous domains. For each domain, the time-averaged parameters of the stress tensor were calculated.

The reconstruction results show that in the study region, as for most subduction zones, the projections of the axes of maximum deviatoric compression σ_3 and tension σ_1 are oriented orthogonally to the strike of the Kuril-Kamchatka Trench (Figure 2), with the compression axis plunging beneath the oceanic plate and the tension axis plunging beneath the continental plate. The intermediate principal stress axis σ_2 is directed along the strike of the Kuril-Kamchatka Trench.

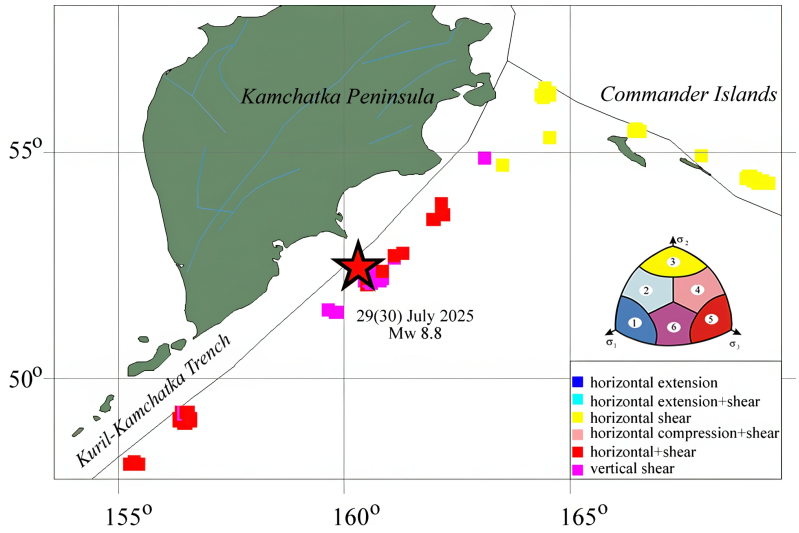

Figure 2. Type of stress state (geodynamic regime).

The axes of the algebraically minimum stress σ_3 plunge gently to the southeast; the plunge of these axes decreases toward the island arc, and in some areas, a reversal of plunge occurs. A rather sharp change in the trend of the σ_3 axes is observed in the junction area of the Kamchatka segment of the seismofocal zone with the Aleutian segment. The axes of the algebraically minimum stress σ_1 here have a steep plunge. Furthermore, large deviations of these axes from the mean trend are observed compared to those for σ_3.

Data on the relationship between the orientation of the principal stress axes and the zenith vector allow for zoning by type of stress state (geodynamic regime). The typical orientation of principal stresses in subduction areas determines the predominant regime of horizontal compression. However, at depths of 0–30 km, at the junction of the Aleutian Arc with the Kuril-Kamchatka segment, an important element of the stress field is the change in the plunge orientation of the axes of maximum deviatoric compression and tension. The environment of horizontal compression gives way to an environment of horizontal shear (Figure 2). This is related to the fact that here the axes of maximum deviatoric compression and tension are oriented at an angle close to 45° to the strike of the Aleutian segment. A strike-slip regime (vertical shear) is also manifested along the Kamchatka coast.

The preparation zone of the strong earthquake of July 29 (30), 2025, M_W 8.8 (focal mechanism type-reverse) within the considered depth interval corresponds to horizontal compression. At the same time, areas of vertical shear are noted here.

The distribution of the Lode–Nadai coefficient values appears homogeneous (Figure 3). The main type of stress tensor in the study area is pure shear, where the algebraically maximum and minimum deviatoric principal stresses are close in absolute value and opposite in sign, and the intermediate deviatoric principal stress is zero. Deviations from this type of tensor (stress ellipsoid) are observed near the junction of the Aleutian and Kamchatka segments with the seismofocal zone; here, pure shear and its combination with uniaxial compression and tension occur. The considered terminal area is characterized by high compressive supra-lithostatic confining pressure. Some weakening of pressure or an increase in maximum shear stresses is observed for the Aleutian segment, where areas of supra-lithostatic confining extension are present [*Rebetsky*, 2007].

The most spatially stable parameter is the orientation of the underthrusting shear stresses. This may indirectly indicate that precisely the underthrusting shear stresses should be considered as the active forces acting on the lithospheric plate from the mantle [*Rebetsky*, 2007]. It is particularly noteworthy that the direction of these stresses is the most stable, even compared to the orientation of the maximum compression stress axes, which allows considering the shear stresses acting on horizontal planes as an active influence forming the stress state in accordance with the structural features of the study area. The

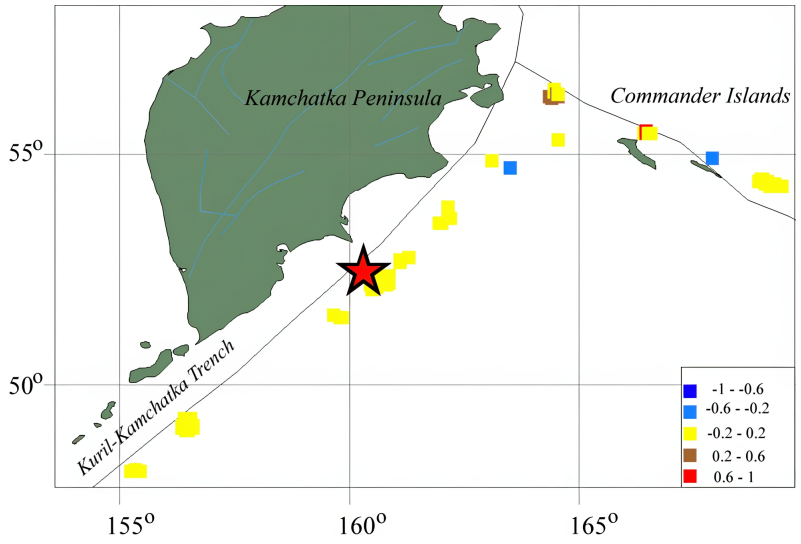

Figure 3. Type of stress tensor Lode–Nadai coefficient.

stable orientation of underthrusting shear stresses acting on horizontal planes in the Earth's crust in the direction from the oceanic plate to the continental plate determines the corresponding type of subcrustal lithospheric substance as the active driving forces of the current stage of the tectonic process. For the Aleutian segment of the Pacific plate boundary, the direction of the underthrusting forces is oblique relative to its strike.

At the second stage of the reconstruction, the results of calculations of the relative values of effective pressure and maximum stress were obtained (Figure 4). In general, the study area is characterized by high values of effective pressure and deviatoric stresses. Such an increase occurs with a more rapid growth of effective pressure [*Rebetsky*, 2007]. The increase in stress intensity near the Earth's crust of Kamchatka is due to the edge effect from the Aleutian Arc. This area, being a zone of dextral shear, forms adjacent sectors of confining compression and tension stresses in its terminal area [*Osokina and Fridman*, 1987]. The compression sector falls on the Kamchatka segment of the seismofocal zone, and the tension sector on the Aleutian segment. However, the depth layer of 0–30 km, in particular, the source preparation zone of the strong earthquake of July 29 (30), 2025, M_W 8.8, is characterized by a relatively low level of effective pressure and maximum shear stress.

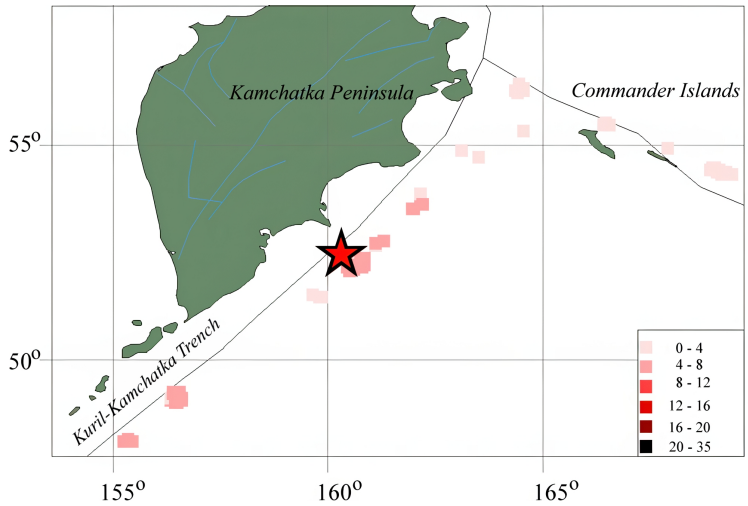

Figure 4. Relative values of effective pressure.

4. Conclusion

The stress reconstruction results obtained for the study region revealed a number of features in the spatiotemporal distribution of the stress state parameters. A similarity between the stress tensors and increments of seismotectonic deformations is characteristic of the study region. Low anisotropy is observed only for the crustal block near the junction of the Aleutian and Kamchatka segments. Based on the analysis of the contemporary stress state, seismotectonic domains with different deformation regimes were identified. An important feature of the stress field is associated with the junction area of the Aleutian and Kamchatka seismofocal zones, where the main heterogeneities of the stress field are observed. The identified features reflect the stress state preceding the strong Kamchatka earthquake over the entire observation period (1974–2025). In the preparation zone of the strong 2025 Kamchatka earthquake, low values of relative effective pressure were noted; such areas, according to the MCA concept, are potentially hazardous areas for their complete failure during the dynamic development of the process.

Acknowledgments. The research was carried out with the financial support of the Ministry of Science and Higher Education of the Russian Federation (state assignments of the Institute of Volcanology and Seismology of the Far Eastern Branch of the Russian Academy of Sciences FWME-2024-0010, Vitus Bering Kamchatka State University FZSS-2025-0007, the Institute of Physics of the Earth of the Russian Academy of Sciences, the Institute of Marine Geology and Geophysics of the Far Eastern Branch of the Russian Academy of Sciences). The GCMT catalog was accessed August 3, 2025, available at http://www.globalcmt.org.

References

Angelier J. Tectonic analysis of fault slip data sets // Journal of Geophysical Research: Solid Earth. — 1984. — Vol. 89, B7. — P. 5835–5848. — https://doi.org/10.1029/jb089ib07p05835

Angelier J. Inversion of earthquake focal mechanisms to obtain the seismotectonic stress IV-a new method free of choice among nodal planes // Geophysical Journal International. — 2002. — Vol. 150, no. 3. — P. 588–609. — https://doi.org/10.1046/j.1365-246x.2002.01713.x

Angelier J. and Mechler P. Sur une methode graphique de recherche des contraintes principales egalement utilisables en tectonique et en seismologie: la methode des diedres droits // Bulletin de la Société Géologique de France. — 1977. — Vol. S7–XIX, no. 6. — P. 1309–1318. — https://doi.org/10.2113/gssgfbull.s7-xix.6.1309 — (In French).

Aprodov V. A. Earthquake Zones. — Moscow : Mysl', 2000. — 461 p. — (In Russian).

Bott M. H. P. The Mechanics of Oblique Slip Faulting // Geological Magazine. — 1959. — Vol. 96, no. 2. — P. 109–117.

Chebrov D. V., Matveenko E. A., Romasheva E. I., et al. Seismicity of Kamchatka and the Commander Islands in 2018-2019 // Earthquakes in Northern Eurasia. — 2023. — No. 26. — P. 171–184. — https://doi.org/10.35540/1818-6254.2023.26.14 — (In Russian).

Chebrov D. V., Saltikov V. A., Matveenko E. A., et al. Seismicity of Kamchatka and the Commander Islands in 2015 // Earthquakes in Northern Eurasia. — 2021. — No. 24. — P. 153–163. — https://doi.org/10.35540/1818-6254.2021.24.14 — (In Russian).

Dobrovolsky I. P. Theory of Tectonic Earthquake Preparation. — Moscow : Nauka, 1991. — 224 p. — (In Russian).

Etchecopar A. Étude des États de Contrainte en Tectonique Cassante et Simulations de Déformations Plastiques: Approche Mathématique : PhD thesis / Etchecopar A. — 1984. — P. 270. — (In French).

Etchecopar A., Vasseur G. and Daignieres M. An inverse problem in microtectonics for the determination of stress tensors from fault striation analysis // Journal of Structural Geology. — 1981. — Vol. 3, no. 1. — P. 51–65. — https://doi.org/10.1016/0191-8141(81)90056-0

Fedotov S. A. and Solomatin A. V. The long-term earthquake prediction for the Kuril-Kamchatka island arc for the April 2016 through March 2021 period, its modification and application; the Kuril-Kamchatka seismicity before and after the May 24, 2013, M 8.3 deep-focus earthquake in the Sea of Okhotsk // Journal of Volcanology and Seismology. — 2017. — Vol. 11, no. 3. — P. 173–186. — https://doi.org/10.1134/s0742046317030022

Fedotov S. A. and Solomatin A. V. Long-Term Earthquake Prediction (LTEP) for the Kuril-Kamchatka island arc, June 2019 to May 2024; Properties of Preceding Seismicity from January 2017 to May 2019. The Development and Practical Application of the LTEP Method // Journal of Volcanology and Seismology. — 2019. — Vol. 13, no. 6. — P. 349–362. — https://doi.org/10.1134/s0742046319060022

Gavrilov V. A., Poltavtseva E. V., Titkov N. N., et al. Monitoring of Changes in the Stress-Strain State of Geoenvironment at the Petropavlovsk Geodynamic Testing Site Based on the Multi-Instrumental Borehole and GPS Data During the Active Phase of Preparing the Zhupanovsky Earthquake (January 30, 2016, Mw 7.2) // Geodynamics & Tectonophysics. — 2023. — Vol. 14, no. 6. — https://doi.org/10.5800/gt-2023-14-6-0732 — (In Russian).

Gephart J. W. Stress and the direction of slip on fault planes // Tectonics. — 1990. — Vol. 9, no. 4. — P. 845–858. — https://doi.org/10.1029/TC009i004p00845

Gephart J. W. and Forsyth D. W. An improved method for determining the regional stress tensor using earthquake focal mechanism data: Application to the San Fernando Earthquake Sequence // Journal of Geophysical Research: Solid Earth. — 1984. — Vol. 89, B11. — P. 9305–9320. — https://doi.org/10.1029/jb089ib11p09305

Gushchenko O. I. Lithosphere seismotectonic stress monitoring (structural and kinetic principle and basic elements of algorithm) // Doklady Akademii Nauk. — 1996. — Vol. 346, no. 3. — P. 399–402. — (In Russian).

Michael A. J. Determination of stress from slip data: Faults and folds // Journal of Geophysical Research: Solid Earth. — 1984. — Vol. 89, B13. — P. 11517–11526. — https://doi.org/10.1029/jb089ib13p11517

Nikitin L. V. and Yunga S. L. Methods for the Theoretical Determination of Tectonic Deformations and Stresses in Seismically Active Regions // Izvestiya AN SSSR. Fizika Zemli. — 1977. — No. 11. — P. 54–67. — (In Russian).

Osokina D. N. and Fridman V. N. Investigation of the laws of the structure of the stress field in the vicinity of a shear discontinuity with friction between the banks // Fields of stresses and deformations in the Earth's crust. — Moscow : Nauka, 1987. — P. 74–119. — (In Russian).

Rebetsky Yu. L. Tectonic Stresses and Strength of Natural Rock Massifs. — Moscow : Akademkniga, 2007. — 406 p. — (In Russian).

Rebetsky Yu. L., Dobrynina A. A. and Sankov V. A. Tectonophysical Zoning of Active Faults of the Baikal Rift System // Geodynamics & Tectonophysics. — 2024. — Vol. 15, no. 4. — https://doi.org/10.5800/gt-2024-15-4-0775 — (In Russian).

Rebetsky Yu. L. and Sycheva N. A. The stressed state of the Earth's crust in the Altai-Sayan mountain region: reconstruction based on the modified algorithms of the cataclastic method // Geosystems of Transition Zones. — 2024. — Vol. 8, no. 4. — P. 261–276. — https://doi.org/10.30730/gtrz.2024.8.4.261-276

Wallace R. E. Geometry of Shearing Stress and Relation to Faulting // The Journal of Geology. — 1951. — Vol. 59, no. 2. — P. 118–130. — https://doi.org/10.1086/625831